NANO LETTERS
2008
Vol. 8, No. 7
2077-2081

On the Polyol Synthesis of Silver Nanostructures: Glycolaldehyde as a Reducing Agent

Sara E. Skrabalak,[†,‡] Benjamin J. Wiley,[†,§] Munho Kim,[||] Eric V. Formo,[||] and Younan Xia*,[||]

Department of Chemistry and Department of Chemical Engineering, University of Washington, Seattle, Washington 98195, and Department of Biomedical Engineering, Washington University, Saint Louis, Missouri 63130

Received April 1, 2008; Revised Manuscript Received May 12, 2008

ABSTRACT

The polyol synthesis is a popular method of preparing metal nanostructures, yet the mechanism by which metal ions are reduced is poorly understood. Using a spectrophotometric method, we show, for the first time, that heating ethylene glycol (EG) in air results in its oxidation to glycolaldehyde (GA), a reductant capable of reducing most noble metal ions. The dependence of reducing power on temperature for EG can be explained by this temperature-dependent oxidation, and the factors influencing GA production can have a profound impact on the nucleation and growth kinetics. These new findings provide critical insight into how the polyol synthesis can be used to generate metal nanostructures with well-controlled shapes. For example, with the primary reductant identified, it becomes possible to evaluate and understand its explicit role in generating nanostructures of a specific shape to the exclusion of others.

The polyol synthesis provides a simple and versatile approach to metal nanostructures.[1–8] Despite its success in controlling the size and shape of many noble-metal nanostructures, the fundamental aspect of this synthesis—how metal ions are reduced by ethylene glycol (EG)—remains poorly understood. As a result, it is still unclear why subtle changes to the reaction conditions cause metal atoms to nucleate and grow into nanostructures of different shapes. Here we show, for the first time, that heating EG in air generates the reductant glycolaldehyde (GA) and that the kinetics of this oxidation reaction can be manipulated controllably. These new results provide critical insight into why the polyol synthesis has been so successful in generating metal nanostructures with well-defined and controllable shapes.

Fiévet et al. studied the mechanism of polyol reduction, with a focus on cobalt and nickel hydroxide precursors.[9] On the basis of the detection of diacetyl after reaction at 197 °C, they proposed acetaldehyde as a possible reductant

$$\mathrm{HOCH_2CH_2OH} \rightarrow \mathrm{CH_3CHO} + \mathrm{H_2O} \qquad (1)$$

$$2\mathrm{M}^+ + 2\mathrm{CH_3CHO} \rightarrow \mathrm{CH_3COCOCH_3} + 2\mathrm{M} + 2\mathrm{H}^+ \qquad (2)$$

While not discussed in their paper, acetaldehyde production was likely promoted by the hydroxide anions from the metal precursors and thus cannot account for the general reductive power of EG under most reaction conditions.[10] Additionally, this mechanism fails to explain the following observations: (i) no diacetyl was detected at 150 °C, but reduction of many metal precursors still occurs and (ii) the reduction rate is highly dependent on the reaction atmosphere. Thus, alternative pathways must exist. For example, heating EG in air may generate GA, a reductant for many metal ions

$$2\mathrm{HOCH_2CH_2OH} + \mathrm{O_2} \rightarrow 2\mathrm{HOCH_2CHO} + 2\mathrm{H_2O} \qquad (3)$$

In this study, we consider this reaction pathway and its contribution to the polyol synthesis of Ag nanostructures with controllable shapes.

NMR and gas chromatography−mass spectrometry proved unsuitable for confirming GA production and quantifying its concentration.[11] Thus, we relied on an established spectrophotometric method that involves the oxidation of GA to glyoxal by perchloric acid in the presence of 2,4-dinitrophenylhydrazine (DNPH) to form glyoxal bis-2,4-dinitrophenylhydrazone.[12] Specifically, 1 mL of analyte is added to 5 mL of DNPH solution (0.044 g of DNPH in 57 mL of 70% perchloric acid and 32 mL of water) and 20 mL of water, boiled for 1 h, then cooled with ice. The hydrazone is then extracted with benzene (20 mL then an additional 5 mL), and the solution is made alkaline with sodium ethoxide solution (10 mL of 2.9 g of sodium ethoxide in 100 mL of ethanol). The resulting emulsion is diluted with 20 mL of ethanol and centrifuged to increase its optical transparency, and then an absorbance spectrum is taken. As shown in Figure 1A, this method distinguishes glyoxal from acetal-

---

* Corresponding author, xia@biomed.wustl.edu.

[†] These two authors contributed equally to this work.

[‡] Department of Chemistry, University of Washington.

[§] Department of Chemical Engineering, University of Washington.

[||] Department of Biomedical Engineering, Washington University.

10.1021/nl800910d CCC: $40.75

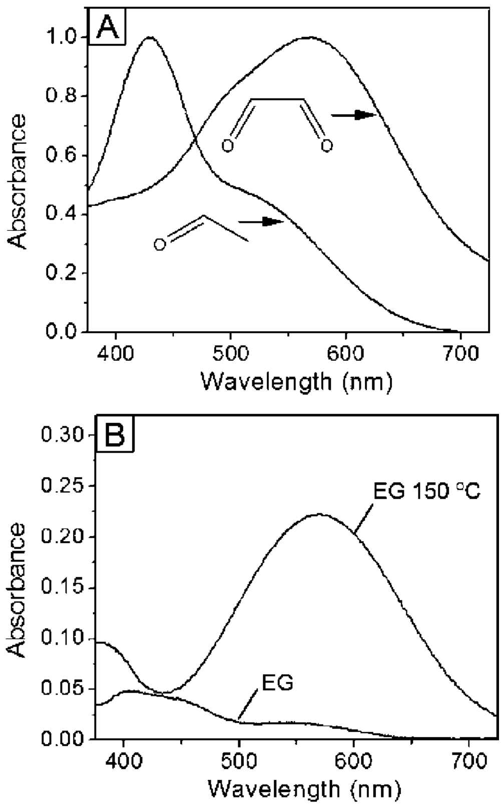

Figure 1. (A) Normalized spectra from tests on 1 mM solutions of acetaldehyde and glyoxal with 2,4-dinitrophenylhydrazine as an indicator. (B) The same test performed on the as-purchased EG and EG after heating at 150 °C for 1 h. The glyoxal peak indicates that glycolaldehyde, $HOCH_2CHO$, was generated upon EG heating.

dehyde (both analyzed as 1 mM EG solutions). Absorbance spectra (Figure 1B) taken after testing as-obtained EG and EG heated at 150 °C in air for 1 h indicate that GA was generated predominately, not acetaldehyde. One can be assured that the peak at 570 nm corresponds to GA production, not glyoxal, because the oxidation of EG to glyoxal requires both heat and nitric acid.[13]

To ensure GA is generated via air oxidation and not another mechanism,[14,15] Ar-saturated and O_2-saturated EG were heated at 150 °C for 1 h under a continuous flow of either Ar or O_2 and then evaluated. As shown in Figure 2A, saturating EG with Ar completely suppresses GA production while saturating EG with O_2 enhances it. These results are consistent with air oxidation of EG to GA. These results also qualitatively explain the differences in precursor reduction rate observed when the reaction atmosphere is changed (Figure 2B), i.e., increasing the O_2 concentration increases the GA concentration, which in turn, increases the amount of precursor that can be reduced. Note that when O_2 is completely excluded from a reaction, reduction of $AgNO_3$ still occurs, albeit at a much slower rate (Figure 2B). This observation can be attributed to EG (or possibly poly(vinyl pyrrolidone), PVP), a much weaker reducing agent than GA.[16] Given that EG is a weaker reductant than GA, when both are present in significant quantities (i.e., at 150 °C under air), GA will be the primary reductant.

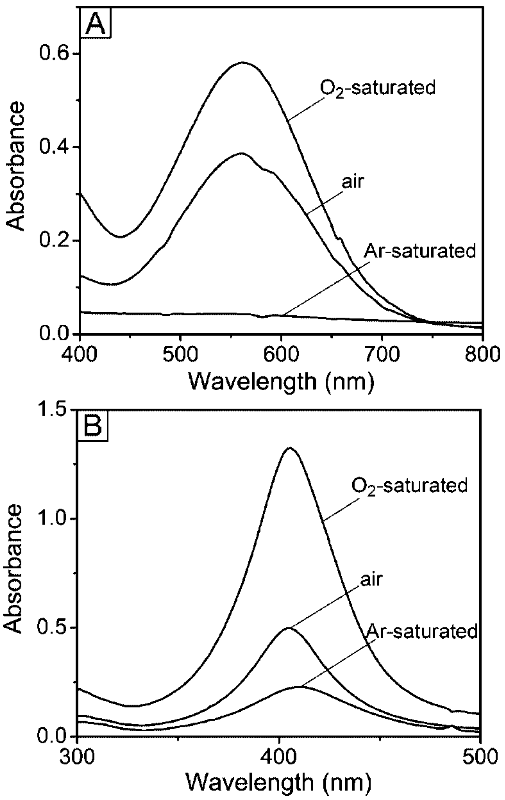

Figure 2. (A) Spectra indicating the amount of GA produced from heating (150 °C for 1 h) as-purchased EG, O_2-saturated EG, and Ar-saturated EG; heating was performed under the indicated atmosphere, and background GA from the colorimetric test was subtracted from all spectra. (B) Spectra of Ag nanoparticles produced after the addition of PVP and $AgNO_3$ to EG (air, O_2-, or Ar-saturated) that was heated at 150 °C for 1 h. EG heating was stopped just before the addition of $AgNO_3$ solution, and the final products were diluted to 25 mL for analysis. In the absence of O_2, EG itself (or possibly PVP) is likely responsible for metal precursor reduction.

If GA is the primary reductant, its concentration should decrease through reaction with the metal precursor. To verify this point, $AgNO_3$ solution (1 mL of EG containing 0.12, 0.06, or 0.03 g of $AgNO_3$) was added to EG (5 mL) that was heated at 150 °C in air for 1 h; the heating ceased immediately prior to $AgNO_3$ addition to minimize continued GA production. After the generated Ag was removed by centrifugation, the EG was tested for GA and compared to when a blank solution was added to the heated EG. Figure 3A shows that the signal from the spectroscopic test decreased slightly relative to the control when a moderate amount of $AgNO_3$ (0.03 or 0.06 g of $AgNO_3$ in 1 mL of EG) was added to the heated EG. Yet, the signal did not continue to decrease when more $AgNO_3$ was added. Rather, the signal exceeded the control when the amount of $AgNO_3$ was increased to 0.12 g. This observation indicates that more GA must be produced during the course of reaction. As shown later, the Ag nanoparticles produced during polyol reduction can catalyze the oxidation of EG to GA (and likely other EG oxidation products).

The catalytic properties of Ag nanoparticles in solution are interesting; however, they also limit our ability to quantitatively demonstrate the 1:1 relationship between the reductant and oxidant. To circumvent this limitation, the

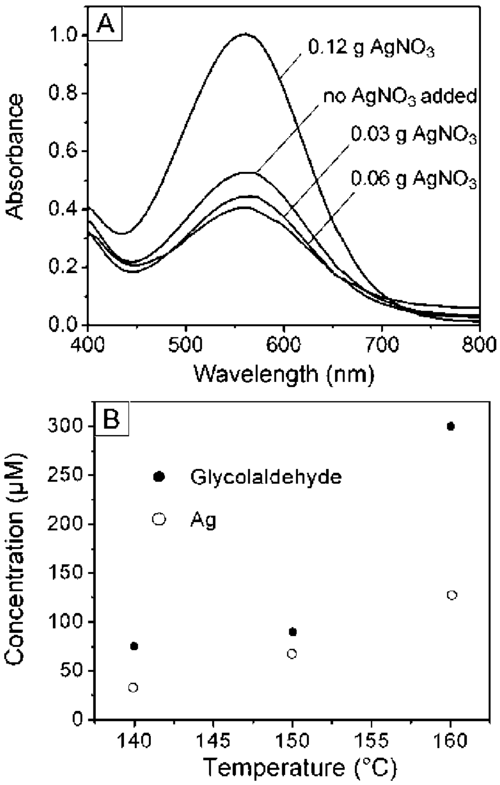

Figure 3. (A) Spectra from the colorimetric test on EG to which $AgNO_3$ solution (0, 0.03, 0.06, 0.12 g of $AgNO_3$ in 1 mL of EG) was added after heating 5 mL of EG at 150 °C in air for 1 h. (B) The concentration of GA generated in EG after 1 h at a given temperature is compared to the amount of $AgNO_3$ reduced.

amount of GA produced immediately prior to reaction was measured and compared to the amount of $AgNO_3$ reduced. If GA is the primary reductant, its concentration should always be greater than or equal to that of the metal precursor reduced. Solutions of PVP (1 mL of EG containing 0.0306 g of PVP $M_w \approx 55000$) and $AgNO_3$ (1 mL of EG containing 0.0306 g of $AgNO_3$) were sequentially added to EG (5 mL) that had been heated for 1 h in air; the EG was removed from heat a few seconds before $AgNO_3$ addition so the amount of Ag generated would be representative of the amount of reductant. Spectra of the Ag nanoparticle suspensions produced at 140, 150, and 160 °C indicate that more $AgNO_3$ was reduced as temperature increased (Figure S1A), just as more GA was generated (Figure S1B). For quantitative analysis, calibration curves were constructed from standards to convert peak intensity to concentration (Figure S2). Figure 3B plots the concentrations of GA produced and $AgNO_3$ reduced versus temperature. As would be expected for the reductant, the GA concentration was always just slightly greater than that of $AgNO_3$ reduced to Ag. Additionally, while the temperature-dependent reducing power of EG was recognized in previous work, the chemical mechanism behind it was unresolved because the reductant was unknown. For the temperature range of 140−160 °C, our data attributes it to the thermally driven oxidation of EG to GA. Note that at 120 °C and below, no GA above the background level from the spectroscopic test was detected and precursor reduction was greatly diminished.

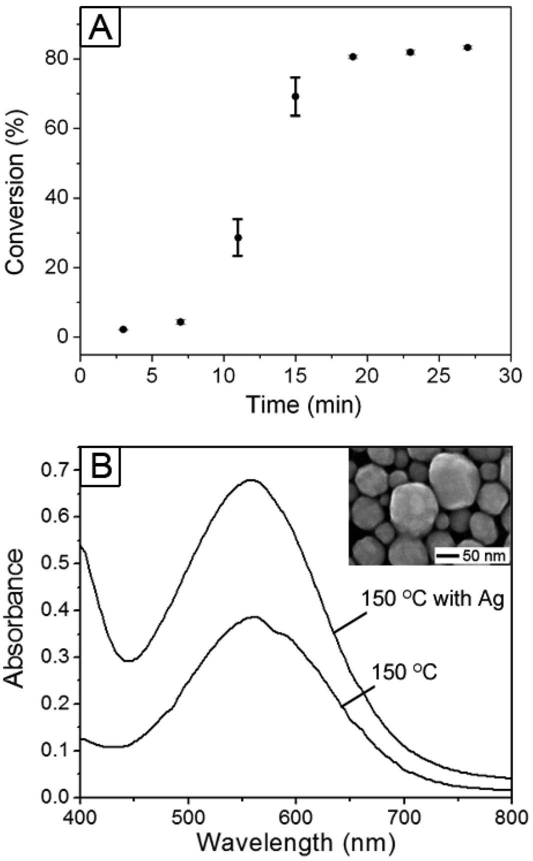

Figure 4. (A) $AgNO_3$ reduction vs reaction time in EG heated at 150 °C in air. Error bars represent the standard deviation of three reactions. (B) Spectra from the colorimetric tests on EG heated at 150 °C for 1 h in air with and without Ag nanoparticles. Background GA from the colorimetric test was subtracted from all spectra. Inset: SEM image of the Ag nanoparticles.

With the primary reductant identified, it becomes possible to evaluate its role in generating nanostructures of specific shapes. As established, the shapes of final products are determined by the rate at which metal atoms add to metal clusters (fluxional assemblies) to form seeds (nonfluxional), the structures of these initial seeds (twinned vs single crystal), the rate at which metal atoms add to seed faces, and the binding selectivity of capping agents.[1,2] The rates at which metal atoms form and assemble are sensitive to reduction kinetics,[17,18] which in turn are dependent on the reductant. To examine the Ag^+ reduction rate, solutions of $AgNO_3$ (1 mL of EG containing 0.0306 g of $AgNO_3$) and PVP (1 mL of EG containing 0.0306 g of PVP $M_w \approx 55000$) were added to EG (5 mL) that was heated for 1 h at 150 °C in air; standard inductively coupled plasma atomic emission spectroscopy techniques were then used to measure the amount of Ag generated. Figure 4A plots the percent conversion as a function of time, where the sigmoidal-shaped curve indicates autocatalytic reduction.

Autocatalytic reduction of noble metal ions has been reported previously in pulse radiolysis studies and was attributed to differences in redox potential as metal clusters grew.[19–21] In the polyol synthesis, this phenomenon could be responsible for the observed autocatalytic reduction. Silver, however, is also known to catalyze EG oxidation to

GA in the gas phase by providing a surface to activate and dissociate O_2.[22] Thus, Ag nanoparticles generated in solution may also catalyze this reaction and be responsible for the autocatalytic reduction of $AgNO_3$ by generating more reductant.[23] To test this hypothesis, Ag nanoparticles prepared by polyol reduction (Figure 4B, inset) were washed, added to fresh EG, and heated at 150 °C in air for 1 h. The EG was then separated from the Ag nanoparticles and tested for GA. Clearly, the signal from the spectroscopic test was greatly enhanced due to the presence of Ag nanoparticles, indicating an increase in GA production, and possibly glyoxal or glyoxylic acid formation (Figure 4B). When EG was heated under Ar, the Ag nanoparticles did not facilitate more GA production, which agrees with the mechanism for Ag-catalyzed EG oxidation.[24] This catalytic generation of reductant raises new possibilities for explaining the formation of nanostructures with different shapes. For example, if a particular crystal plane accelerates EG oxidation more than others, the higher local GA concentration could result in faster metal addition to that plane and thus different morphologies for the final products.

Still, to achieve one structure exclusively, ionic species often have to be added to a polyol synthesis. The roles of such additives are hypothesized in the initial reports,[25–27] but with the reductant identified, we decided to study the effect of these additives on GA production to see if new insight could be gained. For example, we considered the effect of $Fe(NO_3)_3$ which was previously shown to facilitate Ag nanowire growth by accelerating the reduction of $AgNO_3$ and subsequent addition of Ag atoms to the {111} facets of decahedral seeds produced preferentially in most EG-based Ag syntheses.[25] The conditions of EG heating and $Fe(NO_3)_3$ addition mimicked those needed to attain Ag nanowires predominately, but PVP and $AgNO_3$ were omitted to simplify the analysis. Specifically, EG (5 mL) was heated at 160 °C for 1 h in air. Then, 3 mL of EG and 3 mL of 8.06 μM $Fe(NO_3)_3$−EG were added simultaneously at a rate of 45 mL/h. An aliquot was removed 1.5 min after $Fe(NO_3)_3$ addition and tested for GA. In the control, $Fe(NO_3)_3$ was omitted from the second solution. As Figure 5A shows, the addition of Fe(III), a known oxidant, was found to increase GA production.[15,28] This increase in the GA concentration was previously unknown and provides a potential chemical basis for the enhanced reduction of $AgNO_3$. Without this accelerated growth (and possibly the generation of Fe(II), a potential O_2 scavenger), the decahedral seeds would be dissolved by oxidative etching and single-crystal Ag nanostructures would result. In another example, $CuCl_2$ was previously shown to facilitate Ag nanowire growth, and like $Fe(NO_3)_3$, it also enhances GA production (Figure S3).[26,29]

In a third study, we looked at GA production in the presence of Na_2S, which facilitates Ag nanocube growth.[27] The conditions of EG heating and Na_2S addition mimicked those needed to attain Ag nanocubes exclusively, but again, PVP and $AgNO_3$ were omitted to simplify analysis. Specifically, EG (6 mL) was heated in air at 150 °C for 1 h. Then, Na_2S−EG solution (90 μL of a 3 mM solution) was added and heated for 9 min, at which point an aliquot was removed and analyzed. For Ag nanocubes to be produced, cuboctahedron seeds must be generated. Molecular dynamic simulations show that the twin structure of seeds is dependent on reduction rate and that single-crystal cuboctahedron structures will be favorable if Ag atom addition to initial Ag clusters is suitably fast.[30,31] For the Na_2S-mediated polyol synthesis, Ag nanocubes are produced presumably by meeting this condition; however, direct evidence for the chemical basis of this fast reduction has not been provided.[27] As Figure 5B indicates, however, this phenomenon cannot be from increased GA, which in turn supports our hypothesis that Na_2S facilitates, upon $AgNO_3$ addition, the formation of Ag_2S, a catalyst for Ag^+ reduction.[32]

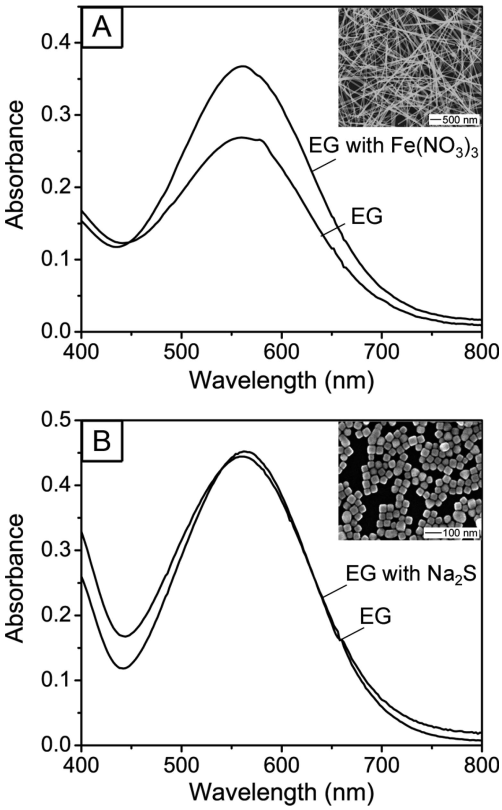

Figure 5. (A) Spectra from the colorimetric tests on EG heated at 160 °C for 1 h in air with and without $Fe(NO_3)_3$. Inset: SEM image of Ag nanowires. (B) Spectra from the colorimetric tests on EG heated at 150 °C for 1 h in air with and without Na_2S. Inset: SEM image of Ag nanocubes. Background from the colorimetric test was subtracted from all spectra.

In conclusion, GA is formed upon EG heating in air to become a dominant reductant for polyol syntheses of Ag nanostructures. By identifying GA as a reductant and understanding the conditions that influence its production (i.e., temperature, atmosphere and experimental setup, additives, EG impurities), we have gained critical insight into how the kinetics of this oxidation reaction might be manipulated controllably to produce metal nanostructures with different shapes. This knowledge may also enhance the reproducibility and scalability of polyol syntheses of metal nanocrystals. Although this study focused on Ag, GA is likely the primary reductant in polyol syntheses for other noble metals when the reaction temperature is between 140 and 160 °C. At lower temperatures, EG as a reductant itself becomes more significant. This difference in the reductant at different reaction temperatures is important because Pd and Pt nanocrystals are usually prepared at lower temperatures than polyol syntheses of Ag nanocrystals. In practice, Pt and Pd precursors have proven to be more easily reduced than Ag precursors, thus it is unsurprising that ethylene glycol itself is sufficient.[33–35] Such information may prove invaluable to experimentalists trying to determine the optimal conditions for the polyol synthesis of different metal nanocrystals. Thus, further elucidation of this chemistry will deepen our understanding of how atoms assemble into nanostructures of specific shapes.

Acknowledgment. This work was supported by NSF (DMR-0451788). Y.X. is a Camille Dreyfus Teacher Scholar. B.J.W. was also partially supported by an IGERT Fellowship from the Center for Nanotechnology funded by NSF and NCI.

Supporting Information Available: Descriptions of experimental details and data analysis, spectra of AG nanoparticles, and colorimetric tests. This material is available free of charge via the Internet at http://pubs.acs.org.

References

(1) Wiley, B. J.; Sun, Y.; Xia, Y. *Acc. Chem. Res.* **2007**, *40*, 1067.
(2) Xiong, Y.; Xia, Y. *Adv. Mater.* **2007**, *19*, 3385.
(3) Kim, F.; Connor, S.; Song, H.; Kuykendall, T.; Yang, P. *Angew. Chem.* **2004**, *28*, 3759.
(4) Kim, F.; Connor, S.; Song, H.; Kuykendall, T.; Yang, P. *Angew. Chem., Int. Ed.* **2004**, *43*, 3673.
(5) Hoefelmeyer, J. D.; Niesz, K.; Somorjai, G. A.; Tilley, T. D. *Nano Lett.* **2005**, *5*, 435.
(6) Caixia, K.; Zhu, X.; Wang, G. *J. Phys. Chem. B* **2006**, *110*, 4651.
(7) Chen, J.; Wiley, B. J.; Xia, Y. *Langmuir* **2007**, *23*, 4120.
(8) Fievet, F.; Lagier, J. P.; Figlarz, M. *MRS Bull.* **1989**, *14*, 29.
(9) Blin, B.; Fievet, F.; Beaupère, D.; Figlarz, M. *Nouv. J. Chim.* **1989**, *13*, 67.
(10) Sung, K. *J. Mol. Struct.* **1999**, *468*, 105.
(11) See Supporting Information.
(12) Basson, R. A.; Du Plessis, T. A. *Analyst* **1967**, *92*, 463.
(13) Boese, A. B.; Fink, C. K. In *Glycols*; Curme, G. O., Jr., Johnston, F., Eds.; Reinhold Publishing Corp.: New York, 1952; pp 125−126.
(14) Szammer, J.; Jaky, M.; Gerasimov, O. V. *Int. J. Chem. Kinet.* **1992**, *24*, 145.
(15) Yoshida, E.; Takata, T.; Endo, T. *Macromolecules* **1992**, *25*, 7282.
(16) Xiong, Y.; Washio, I.; Chen, J.; Cai, H.; Li, Z.-Y.; Xia, Y. *Langmuir* **2006**, *22*, 8563.
(17) Baletto, F.; Mottet, C.; Ferrando, R. *Phys. Rev. Lett.* **2000**, *84*, 5544.
(18) Baletto, F.; Rapallo, A.; Rossi, G.; Ferrando, R. *Phys. Rev. B* **2004**, *69*, 235421.
(19) Huang, Z.-Y.; Mills, G.; Hajek, B. *J. Phys. Chem.* **1993**, *97*, 11542.
(20) Henglein, A. *Chem. Rev.* **1989**, *89*, 1861.
(21) Watzky, M. A.; Finke, R. G. *J. Am. Chem. Soc.* **1997**, *119*, 10382.
(22) Voronova, G. A.; Vodyankina, O. V.; Belousova, V. N.; Berzukov, E. V.; Kurina, L. N. *Kinet. Catal.* **2003**, *44*, 652.
(23) Yang, Z.; Li, J.; Yang, X.; Xie, X.; Wu, Y. *J. Mol. Catal. A* **2005**, *241*, 15.
(24) Knyazev, A. S.; Boronin, A. I.; Koshcheev, S. V.; Salanov, A. N.; Vodyankina, O. V.; Kurina, L. N. *Kinet. Catal.* **2003**, *44*, 408.
(25) Wiley, B.; Sun, Y.; Xia, Y. *Langmuir* **2005**, *21*, 8077.
(26) Korte, K. E.; Skrabalak, S. E.; Xia, Y. *J. Mater. Chem.* **2008**, *18*, 437.
(27) Siekkinen, A. R.; McLellan, J. M.; Chen, J.; Xia, Y. *Chem. Phys. Lett.* **2006**, *432*, 491.
(28) After $Fe(NO_3)_3$ addition, the EG appeared faint yellow. UV−vis spectroscopy suggests that glyoxal was formed. This observation is unsurprising given the oxidative power of $Fe(NO_3)_3$. Also note that Fe is a common impurity in EG due to its storage in stainless steel drums. Thus, it is best to select high-quality EG with low Fe content.
(29) As discussed in ref 19, redox active metal ions such as Cu(I) may be capable of reducing Ag(I) when silver clusters are of a critical size; however, the role of GA as a reductant under all reaction conditions and its generation via additive oxidation cannot be dismissed.
(30) Cleveland, C.; Landman, U. *J. Chem. Phys.* **1991**, *94*, 7376.
(31) Mottet, C.; Goniakowski, J.; Baletto, F.; Ferrando, R.; Treglia, G. *Phase Transitions* **2004**, *77*, 101.
(32) Kryukov, A.; Stroyuk, A.; Zin'chuck, N.; Korzhak, A.; Kuchmii, S. *J. Mol. Catal.* **2004**, *221*, 209.
(33) Xiong, Y.; Cai, H.; Wiley, B. J.; Wang, J.; Kim, M. J.; Xia, Y. *J. Am. Chem. Soc.* **2007**, *129*, 3665.
(34) Chen, J.; Wiley, B. J.; McLellan, J.; Xiong, Y.; Li, Z.-Y.; Xia, Y. *Nano Lett.* **2005**, *5*, 2058.
(35) Skrabalak, S. E.; Chen, J.; Sun, Y.; Lu, X.; Au, L.; Cobley, C.; Xia, Y. *Acc. Chem. Res.* **2008**, *41*, in press.

NL800910D